UFIR Smoothing in State Space for T-wave Features Analysis

CARLOS LASTRE-DOMINGUEZ, YURIY S. SHMALIY, OSCAR IBARRA-MANZANO
Universidad de Guanajuato
Dept. of Electronics Engineering
Carretera Valle de Santiago
km 3.5 + 1.8, 36885 Salamanca
MEXICO
{cm.lastredominguez}{ shmaliy }{ ibarrao }@ugto.mx

Abstract: Measurements of electrocardiogram (ECG) signals are widely used in medicine to provide heart diagnosis, because heart diseases are among most frequent causes of death in a modern world. However, measurement noise often makes it difficult to extract features of ECG signals with a sufficient accuracy. Therefore, many investigations were focused on creating effective techniques for features extraction in ECG signals. In this paper, we extract fiducial features of normal and abnormal T-waves of ECG signals using unbiased smoothing filtering in state space. The results are compared to those obtained using the wavelet transform, morphological transform, and threshold-based detection and show that the approach developed has a higher accuracy. It is also shown that unbiased smoothing filtering allows providing an acceptable discrimination between normal and abnormal ECG signals.

Key–Words: ECG signals, unbiased FIR smoothing filter, state-space, features extraction, T-wave.

1 Introduction

In the last decades, the electrocardiogram (ECG) signals have captivated the medical sector by an ability of heart diseases detection. It is known that heart diseases can be learned by tracing changes in the ECG morphological characteristics, such as P-wave, QRS complex and T-wave[1, 2, 3]. In particular, an abnormal T-wave provides information about diseases such as hyperkalemia, heart attack, hypothyroidism, pericardia Chronic myocardial ischemia, and hypertrophy [4, 5]. These diseases can be indicated by investigating the behaviour of T-wave shape [5]. However, if the ECG data are excessively noisy and have artifacts, such an analysis faces difficulties. Therefore, a big attention has been paid during decades to ECG data denoising using appropriate techniques.

There have been proposed a number of diverse methods to denoise ECG data and extract useful features. Some methods, such the Fourier transform-based [6], view ECG signals as stationery and ignore the time resolution. Algorithms based on the wavelets transform provide better results respecting the trade off between the frequency and time [7, 8, 9]. An effectiveness of these methods grows by an appropriate chose of a wavelet function. Also, the Hilbert transform and decomposition methods are used by some authors to learn ECG signals and the machine learning facilities are exploited in [10, 11, 12].

It is known that smoothing is most efficient in signal denoising if some delay-lag is allowed. Because the ECG data analysis is not a strictly real-time process, smoothing can be applied. Specifically, one can employ a polynomial smoother developed by Savitsky and Golay [13] as it is used in many works. A flaw of this smoother is that it relates the q-delay-lag to the middle of the averaging horizon, which is optimal for odd-order polynomials. For even-order polynomials, the Savitsky-Golay smoother is thus not optimal. Although the Savitsky-Golay smoother was optimized in [14, 15] in the minimum mean square error (MSE) sense, it still relies on the middle point of the averaging horizon.

A more general approach is known as the p-shift unbiased finite impulse response (UFIR) filtering developed by Shmaliy *et. al.* [16, 17, 18, 19, 20]. It provides smoothing at any past point on the averaging horizon with a lag $q = -p > 0$ [21, 22, 17]. Therefore, an optimal lag q can be chosen individually for each even-order of the approximating polynomial and not obligatorily at the middle of the averaging horizon, as for the odd-order.

In this paper, we provide denoising and features extraction of ECG data using UFIR smoothing filtering in the state space. In Section 2, a model of the ECG signal is discussed in space state and the UFIR smoothing filter is described. Here, we also describe an iterative UFIR smoothing filtering algorithm and a

propose methodology for fiducial features extraction in T-waves. We base our analysis on the PTB and MIT arrhythmia database available from [23, 24]. In Section 3, validations and comparisons with other methods are provided. Finally, conclusions are drawn in Section 4.

1.1 Fundamental Features of T-wave

The T wave, which is located in the ECG signal after QRS-complex, represents ventricular depolarization. The T wave is coupled with the relative refractory period of ventricular depolarization, which is a period where the cells of heart are vulnerable to the additional stimuli. Therefore, depending on the heart state, the T-wave may demonstrate a regular or irregular behaviour as shown in Fig 1. Under normal conditions, the T-wave is positive. But it can be negative in some leads, such as LIII and precordial leads V1 and V2. Even so, the T-wave can never be negative in LI and LII [4]. It is also known that a peak-point of the T-wave warns about hyperkalemia or myocardial injury, while its inversion means myocardial ischemia.

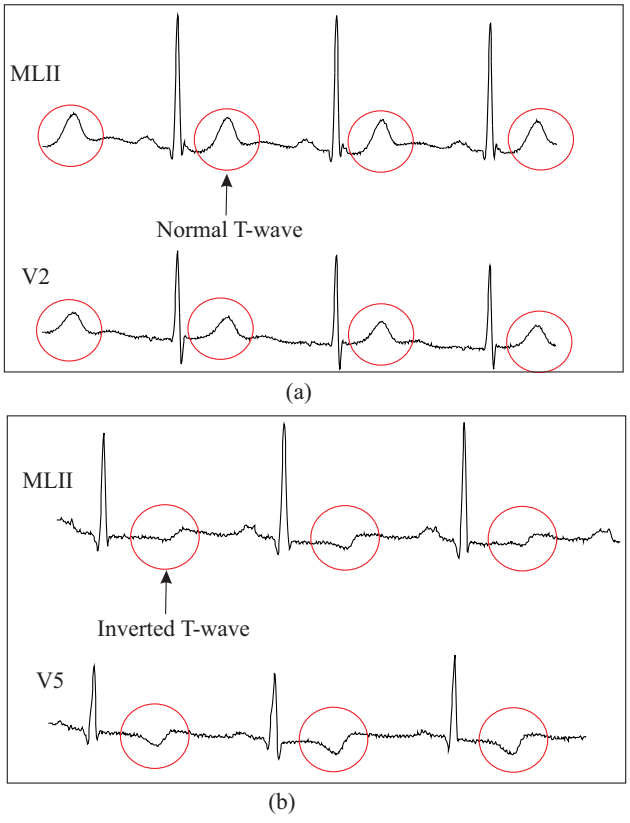

Figure 1: Normal and abnormal shapes of the T-wave.

2 UFIR Approach to T-wave Features Extraction

An UFIR smoothing methodology to the T-wave features extraction is reflected in Fig. (2). Initially, an

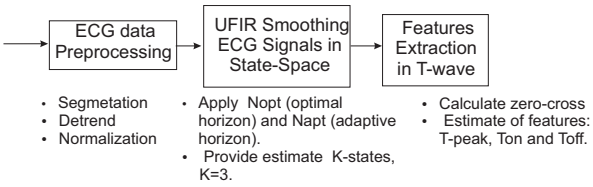

Figure 2: A methodology of the T-wave features extraction using UFIR smoothing.

ECG signal undergoes preprocessing, because it depends of extra factors such as unpredictable movements, shifts of electrodes, and faults of data acquisition system. These and some other factor cause undesirable deviations in the ECG signal difficulties in features extraction. It is thus recommended to provide preprocessing and reduce the ECG signal trend to a zero baseline. In some works, the relevant effect is achieved using linear regression, although a majority of used ECG records do not require a de-trend technique. Of importance also is to keep the same conditions for ECG signals. With this aim, data normalization is commonly provided. Later a signal segmentation is provided as shown by Tompkins in *et. al.* [25]. Provided the preprocessing and segmentation, an UFIR smoother is applied as will be shown next.

2.1 ECG Signal Representation in State Space

By approximating an ECG signal on a horizon of most recent N points with a degree polynomial, the time-invariant deterministic state and noisy measurement equations can be written in discrete time index n as

$$\lambda_n = \mathbf{B}\lambda_{n-1}\,, \tag{1}$$
$$\zeta_n = \mathbf{D}\lambda_n + w_n\,, \tag{2}$$

where $\lambda_n \in \mathbb{R}^K$ is the system state vector, ζ_n is the scalar observation (measurement), $\mathbf{B}_n \in \mathrm{R}^{K\times K}$ represents the system matrix projecting the initial state λ_{n-1} to λ_n,

$$\mathbf{B} = \begin{bmatrix} 1 & \tau & \frac{\tau^2}{2} & \dots & \frac{\tau^{K-1}}{(K-1)!} \\ 0 & 1 & \tau & \dots & \frac{\tau^{K-2}}{(K-2)!} \\ 0 & 0 & 1 & \dots & \frac{\tau^{K-3}}{(K-3)!} \\ \vdots & \vdots & \vdots & \ddots & \vdots \\ 0 & 0 & 0 & \dots & 1 \end{bmatrix}, \tag{3}$$

$\mathbf{D}_n \in \mathrm{R}^{1\times K}$ is the observation matrix,

$$\mathbf{D} = [\,1\;0\cdots 0\,]^T\,, \tag{4}$$

and w_n is the zero mean measurement noise with unknown distribution and statistics. To denoise data and extract ECG signal features, the p-shift UFIR filtering approach can be applied as follows.

2.2 The Batch Unbiased FIR Filter

The batch UFIR filter operates on a horizon $[m, n]$ of N points, from $m = n - N + 1$ to n. To optimize the estimate in the mean square error (MSE) sense, a optimal horizon length $N_{\rm opt}$ is required. This consideration is taken into account only in the slow areas of the ECG signal. Fast ECG signal parts require a minimum horizon, which therefore must be adaptive to avoid large bias errors. Provided a filtering estimate $\hat{\lambda}_n \triangleq \hat{\lambda}_{n|n}$ of λ_n from the past to n, a q-lag smoothing estimate can be calculated by projecting the estimate to $n - q$ as shown in [26].

In a batch form, the UFIR filtering estimate can be written as

$$\hat{\lambda}_n = (\mathbf{H}_{m,n}^T\mathbf{H}_{m,n}^T)^{-1}\mathbf{H}_{m,n}^T\mathbf{Z}_{m,n}\,, \tag{5}$$

where $\mathbf{Z}_{m,n}$ is the observation vector and $\mathbf{H}_{m,n}$ is the measurement matrix, both augmented on a horizon $[m, n]$ as [26]

$$\mathbf{Z}_{m,n} = [\,\zeta_m^T\;\zeta_{m+1}^T\cdots\zeta_m^T\,]^T\,, \tag{6}$$

$$\mathbf{H}_{m,n} = \begin{bmatrix} \mathbf{D}(\mathcal{B}^{m+1})^{-1} \\ \mathbf{D}(\mathcal{B}^{m+2})^{-1} \\ \vdots \\ \mathbf{D}\mathbf{B}^{-1} \\ \mathbf{D} \end{bmatrix}, \tag{7}$$

where $\mathcal{B}$ is a product system matrix specified with

$$\mathcal{B}_r^g = \begin{cases} \mathbf{B}^{r-g+1}\,, & g < r+1\,, \\ \mathbf{I}\,, & g = r+1\,, \\ \mathbf{0}\,, & g > r+1\,. \end{cases} \tag{8}$$

For (6) and (7), the convolution-based batch UFIR filter is given by

$$\hat{\lambda}_n = \mathcal{H}_{m,n}\mathbf{Z}_{m,n}\,, \tag{9}$$

where the gain matrix

$$\mathcal{H}_{m,n} = (\mathbf{H}_{m,n}^T\mathbf{H}_{m,n}^T)^{-1}\mathbf{H}_{m,n}^T. \tag{10}$$

can be rewritten as

$$\mathcal{H}_{m,n} = \mathbf{G}_n\mathbf{H}_{m,n}^T\,, \tag{11}$$

via the generalized noise power gain (GNPG) $\mathbf{G}_n$, which is defined by

$$\mathbf{G}_n = \mathcal{H}_{m,n}\mathcal{H}_{m,n}^T = (\mathbf{H}_{m,n}\mathbf{H}_{m,n})^{-1}\,. \tag{12}$$

Provided the UFIR filtering estimate $\hat{\lambda}_n$, the q-lag UFIR smoothing estimate can be obtained by a projection of

$$\lambda_{n-q|n} = \mathbf{B}^{-q}\lambda_{n|n} \tag{13}$$

and we notice that again that $q = -p$.

2.3 Iterative UFIR Smoothing of ECG Signals

The bach UFIR smoother can also be represented with a computationally efficient iterative algorithm proposed by Shmaliy [27, 26], which pseudo is listed as Algorithm 1. Like the Kalman filter (KF), the iterative UFIR filter provides an estimate in two stages: *predict* and *update*. Iteratively, an estimate $\hat{\lambda}_n$ at time index n is obtained using an auxiliary variable l beginning with $l = m + K$ and ending when $l = n$. The algorithm self-determines the initial state $\hat{\lambda}_{m+K-1}$ at $m + K - 1$ in a batch form on a short horizon $[m, m + K - 1]$, which is required to avoid singularities. It then updates estimates iteratively to reach the best value at n. The estimate $\hat{\lambda}_n$ obtained in such a way with $N_{\rm opt}$ and adaptive horizon $N_{\rm apt}$ minimizes the MSE and is called the optimal UFIR estimate.

Algorithm 1 Iterative UFIR Smoothing Algorithm for ECG Signals

Data: ζ_n , N
Result: $\hat{\lambda}$
Begin :
for $n = N-1, N, \ldots$ **do**
  $m = n - N + 1$, $s = n - N + K$
  $\mathbf{G}_s = (\mathbf{H}_{m,s}\mathbf{H}_{m,s})^{-1}$
  $\tilde{\lambda}_s$= $\mathbf{G}_s(\mathbf{H}_{m,s}^T\mathbf{Z}_{m,s})$
  for $l = s + 1$ to n **do**
    λ_l^-=$\mathbf{B}\lambda_{l-1}$
    $\mathbf{G}_l = [\mathbf{D}^T\mathbf{D} + (\mathbf{B}\mathbf{G}_{l-1}\mathbf{B}^T)^{-1}]^{-1}$
    $\mathbf{K}_l = \mathbf{G}_l\mathbf{D}^T$
    $\tilde{\lambda}_l = \tilde{\lambda}_l^- + \mathbf{K}_l(\zeta_l - \mathbf{D}\tilde{\lambda}_l^-)$
  end for
  $\hat{\lambda}_n$=$\hat{\lambda}_n$
  $\hat{\lambda}_{n-q}$=$\mathbf{B}^{-q}\hat{\lambda}_n$
end for

It is worth mentioning that the UFIR algorithm does not require the noise statistics, which are generally unknown for the heartbeat noise. The the prior

state estimate is predicted by

$$\hat{\lambda}_l^- = \mathbf{B}\lambda_{l-1}\,, \tag{14}$$

the GNPG is updated with

$$\mathbf{G}_l = [\mathbf{D}^T\mathbf{D} + (\mathbf{B}\mathbf{G}_{l-1}\mathbf{B}^T)^{-1}]^{-1}\,, \tag{15}$$

the measurement residual is calculated as

$$z_l = \zeta_l - \mathbf{D}\hat{\lambda}_l^-\,, \tag{16}$$

the bias correction gain is computed by

$$\mathbf{K}_l = \mathbf{G}_l\mathbf{D}^T\,, \tag{17}$$

and the posteriori state estimate is provided by

$$\hat{\lambda}_l = \hat{\lambda}_l^- + \mathbf{K}_l z_l\,. \tag{18}$$

The iterative computation is repeated until $l = n$ and the final values are reflected in the output.

The best accuracy is achieved with Algorithm 1 if $N = N_{\text{opt}}$. To make it possible in the absence of the heartbeat model, we follow [28] and find N_{opt} for ECG signals by minimizing the trace of the derivative of the measurement residual covariance (MRC) matrix $\mathbf{V}(N)$ as

$$\hat{N}_{\text{opt}} = \arg\min_N \frac{\partial\,\text{tr}\mathbf{V}(N)}{\partial N} + 1\,. \tag{19}$$

A solution to the optimization problem (19) has been provided in [29] using an algorithm, which estimates N_{opt}. It was also revealed in [29] for the explored database that $N_{\text{opt}} = 21$ for the 2-degree polynomial corresponding to three states, $K = 3$.

2.3.1 Testing the Iterative UFIR Smoothing Algorithm by ECG Signals

It follows from the ECG signal morphology (Fig. 2) that iterative UFIR smoothing must be organized to have an adaptive averaging horizon. For the 3-state polynomial ECG signal model, the system and measurement matrices can be formed as, respectively,

$$\mathbf{B} = \begin{bmatrix} 1 & \tau & \frac{\tau^2}{2} \\ 0 & 1 & \tau \\ 0 & 0 & 1 \end{bmatrix}\,, \quad \mathbf{D} = [\,1\;0\;0\,]\,, \tag{20}$$

where $\tau = 1/f$ with $f = 360\,\text{Hz}$. Accordingly, the augmented measurement matrix becomes

$$\mathbf{H}_{m,n} = \begin{bmatrix} \mathbf{D}\mathbf{B}^{-2} \\ \mathbf{D}\mathbf{B}^{-1} \\ \mathbf{D} \end{bmatrix}\,. \tag{21}$$

Based on this model and Algorithm 1, the ECG signal features can be extracted as shown below.

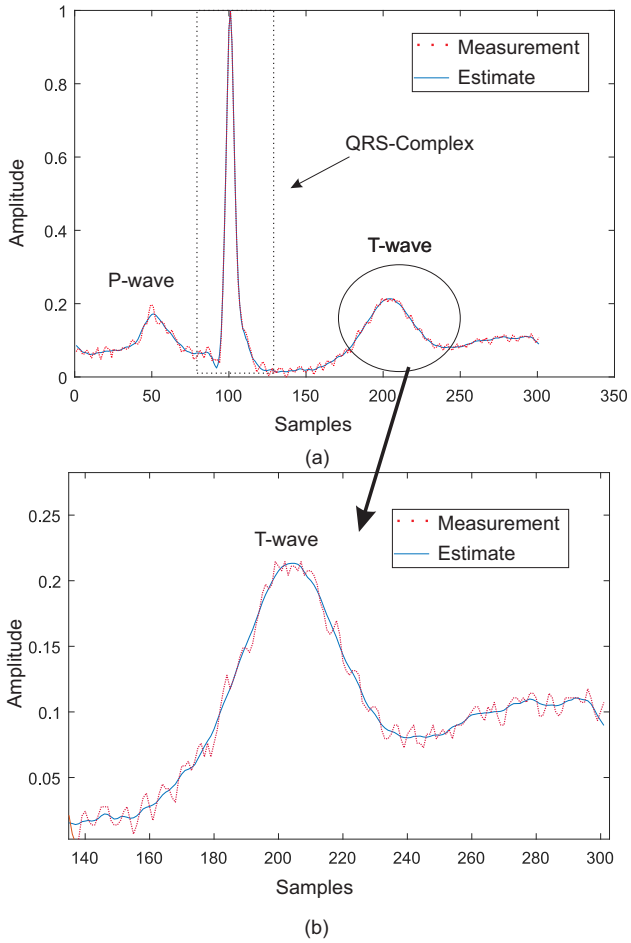

Figure 3: An ECG signal and a T-wave: a) ECG signal estimate (solid) and noisy measurement (dotted), b) T-wave estimate (solid) and noisy measurement (dotted).

2.4 Features Extraction of T-wave

The T-wave features extraction starts with suppressing the P-wave and QRS complex. This part of signal is detected by analysing zero-cross points preceding the T-wave. Detected the P-wave and QRS complex, a new signal is extracted from the ECG signal estimate to contain only the T-wave (Fig.3).

The iterative UFIR smoothing algorithm is next applied to the $K = 3$ model, where the first state represents the T-wave (Dig. 4a), the second state the first time derivative (Fig. 4b), and the third state the second time derivative (Fig. 4c) of the T-wave.

Provided estimates of the T-wave states, features extraction of the T-wave can further be organized as in the following. Points T_{on} and T_{off} are obtained via the peak values, T_{max} and T_{min}. Similarly, features such as the amplitude and duration of the T-wave are calculated: the duration is the difference between T_{off} and T_{on} and amplitude is the difference between a value of the baseline (T_{off} or T_{on}) and a value of

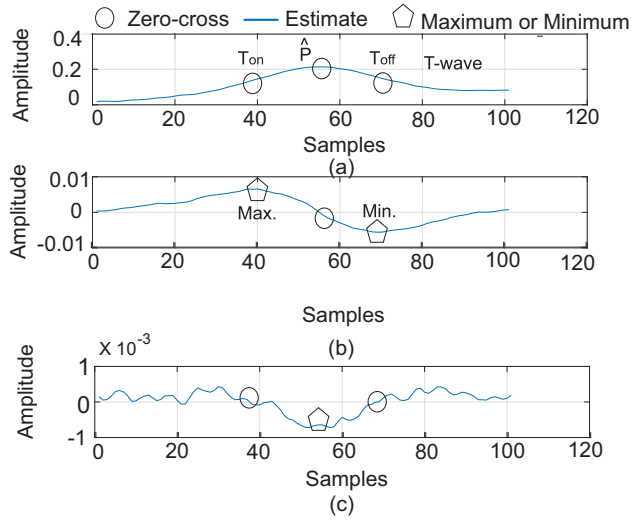

Figure 4: Estimates of the T-wave states provided by the UFIR algorithm: a) first state (smoothed T-wave), b) second state (first time derivative of the T-wave), and c) third state (second time derivative of the T-wave).

the estimated T-peak $\hat{\mathrm{T}}$. This technique is applied to normal and abnormal (inverted) T-waves (Fig. 5).

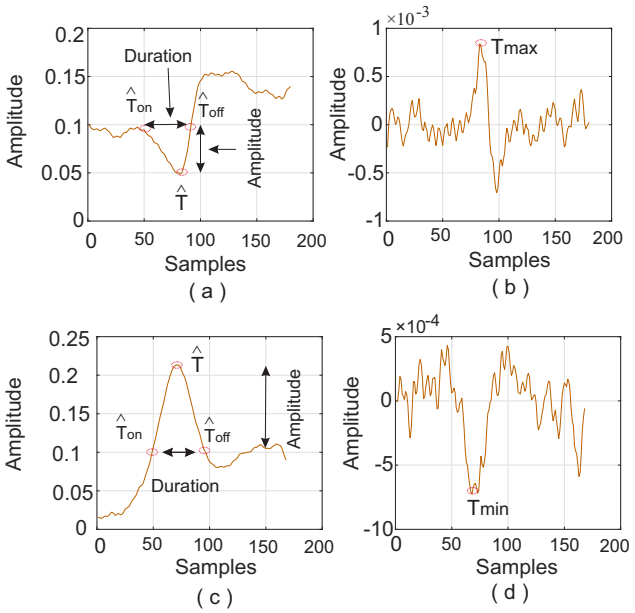

Figure 5: Estimates of the T-peak: a) inverted T-wave, b) third state of the inverted T-wave representing a maximum peak, c) normal T-wave, and d) third state of the normal T-wave representing a minimum peak.

Provided an algorithm for features extraction of the T-wave, the performance of the approach will be discussed next in a comparison with other available methods.

3 Performance of the Proposed Method

The proposed method is validated using the PTB and MIT-arrhythmia database benchmarks, which are recognized as containing records with different diagnosis and pathologies such as arrhythmias, myocardial infarction, heart failure, bundle branch block, myocardial hypertrophy, valvular heart disease, myocarditis, and healthy control. The acceptable tolerances for T-wave are taken from [30].

3.1 A Comparison with Other Methods

Determined T_{on}, the $\mathrm{T}_{\mathrm{off}}$ errors can be computed between the reference pulse and the estimates. The reference value is calculated by approximating an actual one. Errors are averaged to determine the mean value μ and the standard deviation σ.

Table 1 summarizes the results for μ and σ given in milliseconds. In [30], the reference is determined via measurements related to boundaries of the fiducial points. We apply the UFIR-based algorithm and other methods described in the literature; namely, the threshold detector (TD) [31], wavelet detector (WD) [32], and morphological transform (MMD) [33]. As can be seen, the fiducial features estimated using the UFIR-based algorithm and represented with $\mathrm{T}_{\mathrm{off}}$ have the smallest standard deviation indicating that the features are better clustered about the media.

Table 1: ECG Signal Features Extracted Using Different Methods

Method	Parameter	T_{on}	$\mathrm{T}_{\mathrm{off}}$
TD	μ(ms)	23.3	18.7
	σ(ms	28.3	29.8
MMD	μ(ms)	7.9	8.3
	σ(ms	15.8	12.4
WD	μ(ms)	-4.8	-8.9
	σ(ms	13.5	18.8
UFIR	μ(ms)	40.8	10
	σ(ms)	9.63	16.9
CSE(ref)	σ(ms)	–	30.6

3.2 Detection of Abnormalities

Given the MIT-BIH arrhythmia database, we select four records to analyse the amplitude concentration in the T-wave. The first record has an inverted T-wave (Fig 6, circled) that, according to the literature, may be caused by an ischemic heart disease. The second and the third records have normal behaviour. Finally, the fourth record has irregular waves with possible inversions in the T-wave. Known the data conditions shown in Fig. 6, a considerable discrimination can be recognized between the abnormal and normal T-wave.

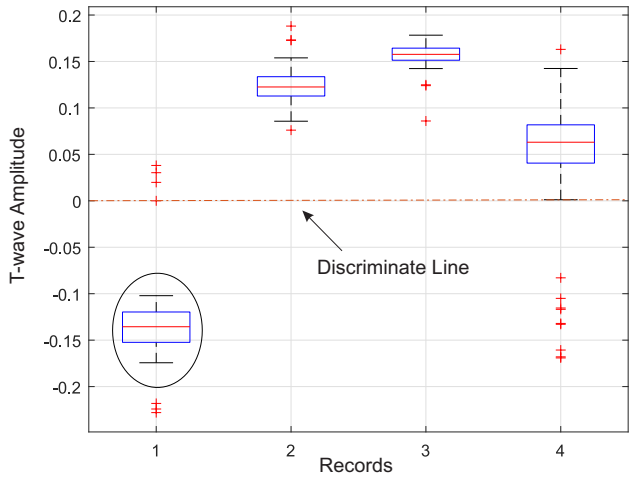

Figure 6: Boxplot of different amplitudes T-waves for different record. A negative amplitude means an inverted T-wave and positive a normal T-wave. The discriminator line is located at zero. The first (circled), second, third, and fourth records are records 100, 101, 103 and 112 in the MIT-Arrhythmia database.

4 Conclusions

A powerful technique employing UFIR smoothing and developed in this paper in state space has shown an important discrimination between the normal and abnormal T-wave shapes. We have designed a method that provides estimation of three ECG signal states: a smoothed signal (first state), its first time derivative (second state), and its second time derivative (third state). A considerable increase in accuracy is achieved as compared to other known techniques of features extraction such as the wavelet transform-based and using a threshold detector. An important result is a detector of the inverted and normal T-waves, which allows determining a notable classification between healthy and sick subjects. As a future work, we are going to extend the algorithm developed to other ECG signal features considering other records with different diseases.

References:

[1] L. Biel, O. Pettersson, L. Philipson, and P. Wide, "ECG analysis: a new approach in human identification," *IEEE Trans. Instrum. Measur.*, vol. 50, no. 3, pp. 808–812, 2001.

[2] L. Smital, V. Martin, J. Kozumplk, and I. Provaznk, "Adaptive wavelet Wiener filtering of ECG signals," *IEEE Trans. Biomed. Eng.*, vol. 60, no. 2, pp. 437–445, 2013.

[3] W. Lu, H. Hou, and J. Chu, "Feature fusion for imbalanced ECG data analysis," *Biomed. Signal Process. Control*, vol. 41, pp. 152–160, 2018.

[4] M. L. Armstrong, *Electrocardiograms: A systematic method of reading them*, 2nd ed., J. Wright and S. Ltd., Eds., Stanford California, United States, 1972.

[5] Z. D. Ary L. Goldberger, Goldberger and A. Shvilkin, *Goldberger's Clinical Electrocardiography*, eigh ed., E. SANDERS, Ed., Philadelphia, PA, United States, 2013.

[6] D. P. Golden, R. A. Wolthuis, and G. W. Hoffler, "A Spectral Analysis of the Normal Resting Electrocardiogram," *IEEE Trans. Biomed. Eng.*, vol. 20, no. 5, pp. 366–372, 1973.

[7] A. D. C. Chan, M. M. Hamdy, A. Badre, and V. Badee, "Wavelet distance measure for person identification using electrocardiograms," *IEEE Trans. Instrum. Measur.*, vol. 57, no. 2, pp. 248–253, 2008.

[8] B. N. Singh and A. K. Tiwari, "Optimal selection of wavelet basis function applied to ECG signal denoising," *Digital Signal Process.*, vol. 16, no. 3, pp. 275–287, 2006.

[9] M. Merah, T. A. Abdelmalik, and B. H. Larbi, "R-peaks detection based on stationary wavelet transform," *Computer Methods and Programs in Biomedicine*, vol. 121, no. 3, pp. 149–160, 2015.

[10] D. Giri, U. R. Acharya, R. Joy, and et al., "Knowledge-based systems automated diagnosis of coronary artery disease affected patients using LDA, PCA, ICA and discrete wavelet transform," *Knowledge-Based Systems*, vol. 37, pp. 274–282, 2013.

[11] R. Joy, U. R. Acharya, K. M. Mandana, A. K. Ray, and C. Chakraborty, "Expert systems with applications of principal component analysis to ECG signals for automated diagnosis of cardiac health," *Expert Systems With Applications*, vol. 39, no. 14, pp. 11 792–11 800, 2012.

[12] I. S. Siva Rao and T. Srinivasa Rao, "Performance identification of different heart diseases based on neural network classification," vol. 11, no. 6, pp. 3859–3864, 2016.

[13] A. Savitzky and M. J. E. Golay, "Smoothing and differentiation of data by simplified least squares procedures." *Analytical Chemistry*, vol. 36, no. 8, pp. 1627–1639, 1964.

[14] S. Hargittai, "Savitzky-Golay least-squares polynomial filters in ECG signal processing," *Computers in Cardiology*, vol. 32, pp. 763–766, 2005.

[15] S. R. Krishnan and C. S. Seelamantula, "On the selection of optimum Savitzky-Golay filters," *IEEE Trans. Signal Process.*, vol. 61, no. 2, pp. 380–391, 2013.

[16] Y. S. Shmaliy, "An unbiased FIR filter for TIE Model of a local clock in applications to GPS-based timekeeping," *IEEE Trans. Ultrason. Ferroelectr. Freq. Control*, vol. 53, no. 5, pp. 862–870, 2006.

[17] Y. S. Shmaliy, O. Ibarra-Manzano, L. Arceo-Miquel, and J. Munoz-Diaz, "A thinning algorithm for GPS-based unbiased FIR estimation of a clock TIE model," *Measurement.*, vol. 41, no. 5, pp. 538–550, 2008.

[18] Y. S. Shmaliy, "An unbiased p-step predictive FIR filter for a class of noise free discrete-time models with independently observed statess," *Signal, Image, Video Process.*, vol. 3, no. 2, pp. 127–135, 2009.

[19] Y. S. Shmaliy, S. Khan, S. Zhao, and O. Ibarra-Manzano, "Ultimate iterative unbiased FIR filtering algorithm," *Measurement*, vol. 92, pp. 236–242, 2016.

[20] ——, "General unbiased FIR filter with applications to GPS-based steering of oscillator frequency," *Measurement*, vol. 25, no. 3, pp. 1141–1148, 2017.

[21] Y. S. Shmaliy and O. Ibarra-Manzano, "Optimal and unbiased FIR filtering in discrete time state space with smoothing and predictive properties," *EURASIP J. Advances Signal Process.*, vol. 2012, no. 1, p. 163, 2012.

[22] Y. S. Shmaliy and L. J. Morales-Mendoza, "FIR smoothing of discrete-time polynomial signals in state space," *IEEE Trans. Signal Process.*, vol. 58, no. 5, pp. 2544–2555, 2010.

[23] A. L. Goldberger, L. A. N. Amaral, L. Glass, and et al., "PhysioBank, PhysioToolkit, and PhysioNet Components of a New Research Resource for Complex Physiologic Signals," *Circulation*, vol. 101, pp. 215–220, 2000.

[24] G. B. Moody and R. G. Mark, "The impact of the MIT-BIH arrhythmia database," *IEEE Eng. Med. Biol. Mag.*, vol. 20, no. 3, pp. 45–50, 2001.

[25] J. Pan and W. J. Tompkins, "A Real-Yime QRS Detection Algorithm," *IEEE Trans. Biomed. Eng.*, vol. BME-32, no. 3, pp. 230–236, 1985.

[26] Y. S. Shmaliy, S. Zhao, and C. Ki Ahn, "Unbiased finite impulse response filtering: an iterative alternative to Kalman filtering ignoring noise and initial conditions," *IEEE Control Syst. Mag.*, vol. 37, no. 5, pp. 70–89, 2017.

[27] Y. S. Shmaliy, "An iterative Kalman-like algorithm ignoring noise and initial conditions," *IEEE Trans. Signal Process.*, vol. 59, no. 6, pp. 2465–2473, 2011.

[28] F. Ramirez-Echeverria, A. Sarr, and Y. S. Shmaliy, "Optimal memory for discrete-time FIR filters in state-space," *IEEE Trans. Signal Process.*, vol. 62, no. 3, pp. 557–561, 2014.

[29] C. Lastre-Dominguez, Y. S. Shmaliy, O. Ibarra-Manzano, and L. J. Morales-Mendoza, "Unbiased FIR denoising of ECG signals," in *2017 14th Int. Conf. Electric. Engineer., Computing Science Automatic Control (CCE)*, no. 1. IEEE, oct 2017, pp. 1–6.

[30] J. Fayn, P. Rubel, and P. W. Macfarlane, "Can the lessons learned from the assessment of automated electrocardiogram analysis in the Common Standards for quantitative Electrocardiography study benefit measurement of delayed contrast-enhanced magnetic resonance images?" *Journal of Electrocardiology*, vol. 40, no. 3, pp. 246–250, 2007.

[31] I. K. Daskalov and I. I. Christov, "Automatic detection of the electrocardiogram T-wave end," *Medical and Biological Engineering and Computing*, vol. 37, no. 3, pp. 348–353, 1999.

[32] C. Li, C. Zheng, and C. Tai, "Detection of ECG characteristic points using wavelet transforms," *IEEE Trans. Biomed. Eng.*, vol. 42, pp. 21–28, 1995.

[33] Y. Sun, K. L. Chan, and S. M. Krishnan, "Characteristic wave detection in ECG signal using morphological transform," *BMC Cardiovascular Disorders*, vol. 5, pp. 1–7, 2005.